

## Nonlinear optical spectroscopy of excited states in disubstituted polyacetylene

C.-X. Sheng,<sup>1,2</sup> M. Tong,<sup>1,\*</sup> and Z. V. Vardeny<sup>1,†</sup><sup>1</sup>Department of Physics & Astronomy, University of Utah, Salt Lake City, Utah 84112, USA<sup>2</sup>School of Electronic and Optical Engineering, Nanjing University of Science and Technology, Nanjing, Jiangsu 210094, China

(Received 14 February 2010; revised manuscript received 25 March 2010; published 4 May 2010)

We used a variety of nonlinear optical (NLO) spectroscopies for studying the excited states order and primary photoexcitations in disubstituted polyacetylene (DPA). The NLO spectroscopies include ultrafast pump-probe photomodulation in a broad spectral range of 0.2–2.5 eV, two-photon absorption in the range of 3.2–4.2 eV, and electroabsorption (EA) in the range of 2.3–4.1 eV. For completeness we also measured the linear-absorption and photoluminescence spectra. We found that the primary photoexcitations in DPA are singlet excitons with *three* photoinduced absorption (PA) bands, PA<sub>0</sub> at 0.6 eV, PA<sub>1</sub> at 1 eV, and PA<sub>2</sub> at 1.6 eV, respectively, and a stimulated emission band at  $\sim 2.5$  eV. This is in contrast to other  $\pi$ -conjugated polymers where the singlet excitons are characterized by *two* PA bands and a stimulated emission (SE) band. We conclude that in addition to the four essential excited states known to determine the NLO spectra of  $\pi$ -conjugated polymers, namely,  $1A_g$ ,  $1B_u$ ,  $mA_g$ , and  $nB_u$ ; in DPA there is another important complex of states at  $\sim 3.3$  eV that contains almost degenerate states with odd and even parity symmetries (dubbed here transverse excited state or TES) that is probably reminiscent of the  $2A_g$  state in unsubstituted *trans*-polyacetylene, which lies in between the  $1B_u$  and  $mA_g$  of which dipole moment has a strong component perpendicular to the chain direction. In support for this model we found that the depolarization ratio of the EA spectrum drastically changes around the TES from a value of  $\sim 2$  for  $\hbar\omega < 3$  eV to  $\sim 0.5$  for  $\hbar\omega > 3.3$  eV.

DOI: 10.1103/PhysRevB.81.205103

PACS number(s): 78.40.Me, 78.40.Fy, 78.40.Pg, 78.47.J–

## I. INTRODUCTION

The photophysics of  $\pi$ -conjugated polymers (PCPs) has been extensively studied for more than two decades. However, the PCP photoexcitations is still hotly debated;<sup>1–7</sup> partly due to the diversity of newly synthesized polymers. Among the class of novel PCPs the disubstituted polyacetylene (DPA) (backbone structure is shown in Fig. 1 inset) is a unique polymer.<sup>8,9</sup> Similar to *trans*-polyacetylene [ $t-(CH)_x$ ], DPA has been shown to have a degenerate ground state<sup>10</sup> that supports soliton excitations.<sup>11</sup> But in contrast to  $t-(CH)_x$ , DPA has very strong photoluminescence (PL) emission in both solution and film forms, which make it suitable for optoelectronic applications such as light emitting diodes and solid-state lasers.<sup>12,13</sup> The strong PL in DPA compared to the very weak PL in  $t-(CH)_x$  shows that the lowest excited state in the former polymer is  $1B_u$  with *odd* or *ungerade* (u) parity symmetry; otherwise the transition from the lowest lying exciton state to the ground state would be forbidden, and this would have weakened the PL. In contrast, the lowest excited state in  $t-(CH)_x$  is  $2A_g$  with *even* or *gerade* parity symmetry,<sup>14,15</sup> which is relatively strongly coupled to the  $1B_u$  state. Surprisingly the reverse excited state order in DPA compared to  $t-(CH)_x$  is *not in conflict* with its degenerate ground-state property.

Several theories have been advanced for explaining the reverse excited state order in DPA compared to that in  $t-(CH)_x$ .<sup>16–19</sup> One explanation is that the strong electron-electron interaction in this polymer causes delocalization of the excited state among the backbone polyenelike monomers on the chain; but also includes the phenyl side groups (see Fig. 1 inset). This “transverse delocalization,” in turn, pushes up  $E(2A_g)$  above  $E(1B_u)$  resulting in strong PL emission.<sup>19</sup> Although the primary photoexcitations in DPA have been

studied before,<sup>19–21</sup> a complete picture of its excited state order is still lacking; the reason might be the relatively narrow probing spectral range used previously, and the lack of complementary nonlinear optical (NLO) spectroscopy measurements. In particular the unique properties of the DPA excited states and their transverse delocalization properties have not been elucidated as yet.

In the present work we employ a *variety* of NLO spectroscopies for studying the primary photoexcitations and important excited states in DPA polymer film and solution. The NLO spectroscopies include broadband ultrafast pump-probe photomodulation (PM), polarized electroabsorption (EA), and two-photon absorption (TPA). We complete our investigation by comparing the NLO spectra with linear optical measurements that include absorption and PL spectra. TPA spectroscopy is sensitive to excited states with  $A_g$  symmetry; and thus is complementary to linear absorption that probes excited states with  $B_u$  symmetry; whereas EA spectroscopy is

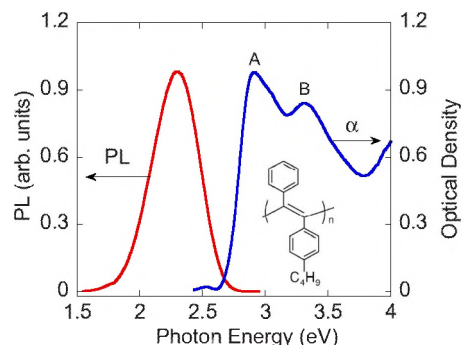


FIG. 1. (Color online) The normalized absorption (blue) and photoluminescence emission (red) spectra of a DPA film. The polymer repeat unit is shown in the inset. Bands A and B are assigned.

sensitive to excited states of both *odd* and *even* symmetries. The application of various NLO and linear spectroscopies to the *same* polymer film, and their polarization dependence have provided us with a more complete picture of the excited states in DPA compared to previous works.<sup>20,21</sup>

In contrast to what is assumed for  $t\text{-(CH)}_x$  (that apparently shows soliton primary photoexcitations) we found that the primary photoexcitations in DPA are *singlet excitons* with odd symmetry. The excitons in DPA are characterized by three correlated transient photoinduced absorption (PA) bands in the mid- and near-IR spectral ranges and a stimulated emission (SE) band in the visible range. Two of the three PA bands can be understood as due to optical transitions in the singlet manifold from  $1B_u \rightarrow mA_g$  ( $PA_1$ ) and  $1B_u \rightarrow kA_g$  ( $PA_2$ ), at 1 eV and 1.6 eV, respectively, and SE from the  $1B_u$  to the ground ( $1A_g$ ) state. This picture is similar to that in many other PCPs, where the excitons were identified as having two PA bands and a SE band.<sup>22</sup> In DPA, however, we found that there is another important excited state complex, dubbed here “transverse excited state” or TES that contains states with odd and even parity symmetries. The TES may explain the third exciton PA band, namely,  $PA_0$  at 0.6 eV as due to the transition  $1B_u \rightarrow \text{TES}$ ; and also the extra band in the linear-absorption spectrum at 3.3 eV. Because the TES dipole moment is mainly perpendicular to the polymer chain, the EA spectrum shows an unusual polarization property. We found that the depolarization ratio, which is defined as the ratio between the fractional change in transmission ( $\Delta T/T$ ) with the polarization of light parallel and perpendicular to the applied electric field, changes from a value of  $\sim 2$  for  $\hbar\omega < 3$  eV to  $\sim 0.5$  for  $\hbar\omega > 3.3$  eV; and the change occurs at the TES photon energy. From our linear and NLO measurements we thus conclude that the lowest intrachain excited state in DPA is a strongly bound exciton ( $1B_u$ ) having an intrachain binding energy of  $\sim 1$  eV; but other excited states above it with less defined symmetry are also important.

## II. EXPERIMENTAL

For the polarized transient PM spectroscopy we used the femtosecond two-color pump-probe correlation technique with two laser systems based on a Ti:Sapphire oscillator<sup>23</sup> a low-power (energy/pulse  $\sim 0.1$  nJ) high-repetition rate ( $\sim 80$  MHz) laser system for the mid-IR spectral range; and a high-power (energy/pulse  $\sim 10$   $\mu$ J) low-repetition rate ( $\sim 1$  kHz) laser system for the near-IR/visible spectral range. For both laser systems the excitation photon energy,  $\hbar\omega$ , was set at 3.1 eV. For the transient mid-IR measurements we used an optical parametric oscillator (Opal, Spectra Physics) that generates  $\hbar\omega$  (probe) from 0.55 to 1.05 eV and from 0.14 to 0.43 eV, respectively.<sup>24</sup> For the transient near-IR measurements, white light supercontinuum was generated having  $\hbar\omega$  (probe) spectrum ranging from 1.15 to 2.7 eV. The transient PM signal,  $\Delta T/T(t)$  is the fractional change,  $\Delta T$  in transmission,  $T$ , which is negative for PA and positive for photobleaching and SE. The transient PM spectra from the two laser systems were normalized to each other in the near-IR/visible spectral range, for which  $\hbar\omega$  (probe) from the low-power laser system was doubled.

The TPA spectrum was measured using the polarized pump-probe correlation technique with the low-repetition rate high-power laser system at time delay  $t=0$ . The linearly polarized pump beam was set at 1.55 eV, which is *below* the polymer absorption band; whereas the probe beam from the white light supercontinuum covered the spectral range from 1.6 to 2.6 eV. The TPA spectrum could be thus obtained in the spectral range of 3.15–4.15 eV. The temporal and spatial overlap between the pump and probe beams on the sample film leads to a PA signal that peaks at  $t=0$ . We interpret it as due to TPA of one pump photon and one probe photon, of which spectrum yields the TPA spectrum. In principle the mid-IR laser system is also capable of producing a TPA contribution to the pump/probe transient PM spectrum at  $t=0$  for  $\hbar\omega$  (pump) at 3.1 eV and  $\hbar\omega$  (probe) in resonance with the most strongly coupled  $mA_g$  state. This can be readily checked by measuring the transient PA decay for  $t>0$ , looking for an ultrafast decay in time that corresponds to the cross-correlation function of the pump and probe pulses. However in our mid-IR measurements we have not detected such a fast decay for the mid-IR PA bands, and this is compelling evidence that these bands are not due to TPA.

For the polarized EA measurements we used a DPA film spin cast on a substrate with patterned metallic electrodes.<sup>25</sup> The EA substrate consisted of two interdigitated sets of a few hundred 30- $\mu$ m-wide gold electrodes, which were patterned on a sapphire substrate. The sample was placed in a cryostat for low-temperature measurements. By applying a potential  $V$  to the electrodes a typical electric field,  $F \sim 10^5$  V/cm was generated with  $V=300$  V and  $f=1$  kHz parallel to the film. For probing the EA spectrum we used an incandescent light source from a Xe lamp, which was dispersed through a monochromator, focused on the sample, and detected by a UV-enhanced silicon photodiode. We measured  $\Delta T$  with probe light parallel and perpendicular to the direction of the applied electric field using a lock-in amplifier set to twice the frequency ( $2f$ ) of the applied field,<sup>25</sup> and verified that no EA signal was observed at  $f$  or  $3f$ .  $\Delta T$  and  $T$  spectra were measured separately and the polarized EA spectrum was obtained from the ratio  $\Delta T/T$ . The detailed description for the EA experimental setup was presented in Ref. 26.

## III. RESULTS AND DISCUSSION

### A. Absorption and PL spectra

Figure 1 shows the optical absorption and PL spectra of a spin cast DPA film. Unlike typical absorption spectra of other PCPs (Ref. 26) that show a single dominant low-energy  $\pi\text{-}\pi^*$  band that follows the absorption edge, the low-energy absorption spectrum in DPA consists of *two* bands at 2.9 eV (A) and 3.3 eV (B), respectively. Band A is assigned as due to the optical transitions from the ground state ( $1A_g$ ) to the first odd-parity exciton ( $1B_u$ ), similar to other PCPs. Band B, however, shows different polarization properties relative to band A,<sup>20</sup> and thus cannot be assigned as due to phonon side band of band A. We thus assign band B to an optical transition from the ground state ( $1A_g$ ) to an excited state of which properties are studied in this work (see below); we dub this complex band as transverse excited state or TES. The PL



spectrum exhibits a featureless band at 2.3 eV with relatively large redshift with respect to the absorption edge.<sup>27</sup> Unlike other luminescent PCPs, the PL spectrum and quantum efficiency ( $\sim 60\%$ ) in DPA are the same in solid film and dilute solution, indicating strong exciton intrachain confinement and weak interchain interaction<sup>28,29</sup> for the polymer in both environments. In addition the PL of a stretched oriented film shows that it is polarized along the polymer chain;<sup>20</sup> thus it originates from the first band in the absorption spectrum (band A), namely, the  $1B_u$   $\pi$ - $\pi^*$  exciton.

### B. Electroabsorption spectroscopy

We applied the EA spectroscopy to elucidate the nature of the excited states responsible for the various absorption bands in the DPA film. EA has provided a sensitive tool for studying the band structure of inorganic semiconductors<sup>30</sup> as well as organic semiconductors.<sup>31–33</sup> In general the EA spectrum emphasizes optical transitions at singularities of the joint density of states that respond sensitively to an external field, and therefore are lifted from the broad background of the absorption continuum.<sup>34</sup> The EA sensitivity, however, diminishes for more confined electronic transitions, because the applied electric fields (on the order of 100 kV/cm) are too small of a perturbation to cause sizable changes in their associated optical transitions. Consequently EA spectroscopy has been an ideal tool to separate exciton bands from the continuum band.<sup>34</sup> For example, in one-dimensional (1D) semiconductors the confined excitons were shown to exhibit a quadratic Stark effect, where the EA signal scales with  $F^2$ , and its spectrum resemble to a first derivative of the absorption edge. Whereas the EA spectrum related to the continuum band was found to scale with  $F^{1/3}$  and showed Franz-Keldysh (FK) type oscillation. In a ground-breaking work, the energy separation of the two distinctive different EA spectral features was therefore used to obtain the exciton binding energy in polydiacetylene, which was found to be  $\sim 0.5$  eV.<sup>34</sup>

Figure 2(a) shows the EA spectrum of a DPA film at 80 K up to 4.1 eV measured at field  $F$  of  $10^5$  V/cm. The EA spectrum scales with  $F^2$  [Fig. 2(b) inset] and thus is due to excitons. There are several prominent spectral features in the EA spectrum: a first-derivative-like feature with zero crossing at  $\sim 2.7$  eV that we assign here as the  $1B_u$ , accompanied by two well-resolved phonon sidebands at 2.77 eV and 2.93 eV, respectively. In addition there are two field-induced absorption bands at higher energies at 3.3 eV and 3.5 eV, respectively. The 3.5 eV field-induced absorption band is assigned as due to oscillator strength given to the  $1A_g \rightarrow mA_g$  transition caused by the symmetry breaking of the polymer chain induced by the strong field. The 3.3 eV field-induced absorption band indicates that an even-symmetry state gains oscillator strength due to the field. Since the 3.3 eV EA band appears at the same energy as band B in the absorption spectrum (Fig. 1), then there is a band at 3.3 eV that contains even and odd states. We thus assigned this band as due to TES with both even and odd parities. The origin of the two parity symmetry could be due to the transverse delocalization nature of states near the TES. At even higher energies

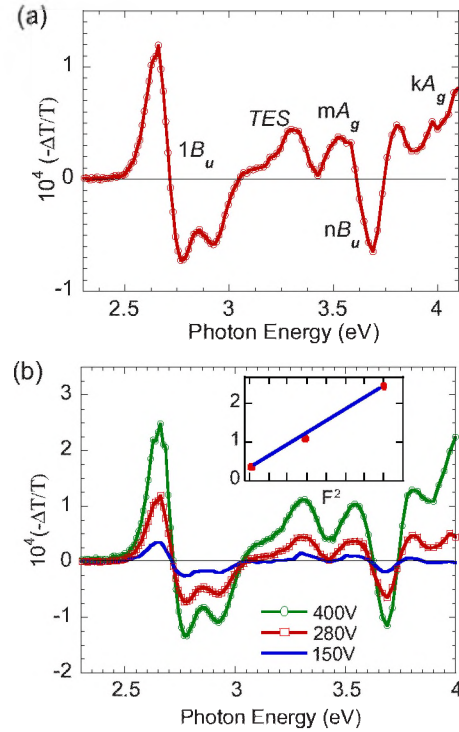


FIG. 2. (Color online) (a) DPA electroabsorption spectrum. The essential states  $1B_u$ ,  $mA_g$ ,  $nB_u$ , and  $kA_g$ , as well as the novel state, TES are assigned. (b) DPA-EA spectrum at three different applied voltages,  $V$  resulting in three different field strengths,  $F$ . The inset shows the linear dependence of the EA signal on  $F^2$ .

the EA spectrum shows a modulation spectral feature that resembles a second derivative with zero crossing at 3.6 eV and 3.8 eV, respectively, these are therefore ascribed to the excited states  $mA_g$  and  $nB_u$  (the latter symbolizes the continuum band threshold in PCPs) that mix under the influence of the electric field; similar to EA spectra in other PCPs.<sup>35</sup> Also above  $E(nB_u)$  there is another field-induced absorption band at  $\sim 3.9$  eV that, similar as in other PCPs we assigned it as due to an even state at higher energies,<sup>26,36</sup> namely, the  $kA_g$ .

No FK-type oscillation related to the onset of the interband transition is seen in the EA spectrum here. The most prominent characteristic properties of a FK oscillation feature is the spectral broadening with the electric field strength  $F$ , and field dependence of  $F^{1/3}$ .<sup>34</sup> Figure 2(b) shows that the EA spectrum does not change much with  $F$ , and also the entire spectrum scales with  $F^2$  [Fig. 2(b) inset]; in contrast to the expectations related to the FK-EA feature. We thus conclude that DPA excited states, including the TES are better described in terms of *excitons*. It is known that the continuum band in PCPs is very close to  $E(nB_u)$ .<sup>33</sup> However, there is no transition around 3.7 eV from the ground state into the continuum band in the linear-absorption spectrum. It is well established in quasi-1D semiconductors that have large exciton binding energy that the interband transition strength substantially decreases relative to the exciton transition strength.<sup>33,34</sup> Here we may estimate the intrachain binding energy,  $E_b$  of the lowest lying singlet exciton in DPA from the relation:  $E_b = E(nB_u) - E(1B_u)$ , which yields  $E_b$

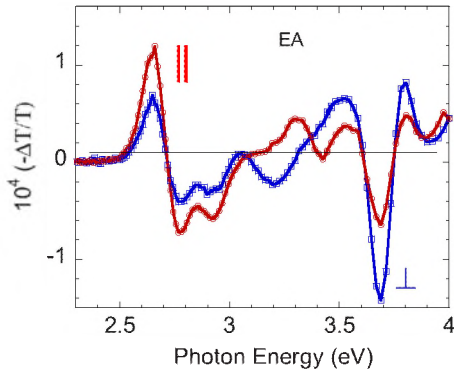


FIG. 3. (Color online) DPA-polarized EA spectrum with light polarization parallel (red) and perpendicular (blue) to the applied electric field direction.

$\approx 1$  eV. This large  $E_b$  is not unique in the class of PCPs (Ref. 25) and is consistent with the unobservable  $1A_g \rightarrow nB_u$  transition in the linear-absorption spectrum (Fig. 1). We therefore conclude that the photophysics of DPA should be also governed by excitons, similar to many other PCPs. We note that soliton excitations were previously observed in PDA films, indicating a degenerate ground state.<sup>10</sup> We emphasize that there is no controversy between the two properties in PDA, namely, the first excited state is a  $1B_u$  exciton, whereas the ground state is still degenerate.<sup>37</sup>

We also measured the polarization dependence of the EA spectrum (Fig. 3); where  $EA_{||}$  ( $EA_{\perp}$ ) stands for the EA component measured with the polarization of the probe light parallel (perpendicular) to the applied electric field direction. It is seen that for  $3 < \hbar\omega < 3.5$  eV the  $EA_{||}$  component shows a field-induced absorption band at 3.3 eV [TES in Fig. 2(a)], however, at the same  $\hbar\omega$  interval the  $EA_{\perp}$  component crosses zero, showing the existence of an odd state similar to the EA spectrum related to  $1B_u$ . This supports our conclusion that the TES band has, in fact, contributions from odd and even parity states that are almost degenerate at  $\sim 3.3$  eV. The distinctive different spectra of the  $EA_{||}$  and  $EA_{\perp}$  components lead to strong variation in the spectrum of the depolarization ratio,  $\rho$  defined as  $\rho = EA_{||}/EA_{\perp}$ . We found  $\rho \sim 2$  for  $\hbar\omega < 3$  eV; but for  $\hbar\omega > 3.3$  eV  $\rho \sim \frac{1}{2}$ . Although the spectra of the two EA components are similar to each other, we found that  $EA_{\perp} > EA_{||}$  in a certain spectral interval, which is quite *unusual* among the EA spectra of PCP.

Electroabsorption is a third-order NLO effect, and thus may be described by the imaginary part of the third-order optical susceptibility, namely,  $\text{Im}[\chi^{(3)}(-\omega; \omega, 0, 0)]$ .<sup>33,38</sup> Therefore, the polarization dependence of the EA spectrum is, in fact, related to the anisotropy of  $\chi^{(3)}$  in the DPA film.  $\chi^{(3)}$  spectrum may be calculated using the summation over states (SOS) model, originally proposed by Orr and Ward,<sup>39</sup> and further developed for  $\pi$ -conjugated polymers by Mazumdar *et al.*<sup>33,38</sup> In this model  $\chi^{(3)}$  spectrum is a summation of 16 terms, each containing a denominator that is proportional to multiplication of several dipole-moment transitions,  $\mu_{ij}$  such as from the ground state,  $1A_g$  to  $1B_u$  ( $1A_g \rightarrow 1B_u$  with strength  $\mu_{01}$ ) and  $1B_u$  to  $mA_g$  ( $1B_u \rightarrow mA_g$  with strength  $\mu_{12}$ ); and a nominator that is at resonance at energies related

to the main essential states [see Eqs. (3)–(12) in Ref. 25]. For traditional PCPs such as poly-p-phenylene vinylene (PPV), the direction of the excited states dipoles is mainly along the polymer chain, which is consistent with the quasi-1D exciton picture in PCPs; this results in a pronounced  $\chi^{(3)}$  anisotropy. In polyfluorene (PFO) film, for example,  $EA_{||}$  is  $\sim 2.1$  larger than  $EA_{\perp}$ ; and the two EA spectra are very similar to each other.<sup>26</sup> However, for DPA at  $\hbar\omega > 3.2$  eV we speculate that the transition dipole moment from the ground state to the corresponding excited state (in this case the  $1A_g \rightarrow TES$  transition; having strength  $\mu_{01}$ ), which resonantly dominates the EA spectrum at these photon energies is *perpendicular* to the polymer chain. Appendix summarizes the depolarization ratio that is obtained in this case.

Also from the form of the  $EA_{\perp}$  spectrum close to  $E(TES)$ , which shows a reverse EA modulation feature compared to that of  $1B_u$  we conclude that there is another strongly coupled  $A_g$  state in DPA, namely,  $2A_g$  with energy  $E(2A_g)$  in between  $E(1B_u)$  and  $E(TES)$ . Its strong coupling with the TES causes the perpendicular Stark shift to be reversed respect to that of the  $1B_u$ . The strong coupling between  $2A_g$  and TES may be tracked back to the strongly coupled  $2A_g$  in unsubstituted polyacetylene.

### C. Two-photon-absorption spectroscopy

In most  $\pi$ -conjugated polymers the allowed optical transitions between the ground state  $1A_g$  and  $B_u$  exciton states, in particular the transition  $1A_g \rightarrow 1B_u$  dominate the absorption spectrum.<sup>40,41</sup> However the one-photon optical forbidden transitions between  $1A_g$  to excited states with  $A_g$  symmetry are optically allowed in TPA process.<sup>38</sup> Therefore TPA spectroscopy has been used in the class of PCPs to study the important  $A_g$  energies.<sup>40,41</sup> Typically two prominent bands dominate the TPA spectrum in PCPs, namely, the  $mA_g$  and  $kA_g$ , where  $E(mA_g) < E(kA_g)$ ;<sup>42</sup> it is thus interesting to investigate the TPA spectrum in DPA because of the important role of the TES in NLO of this polymer.

In this work we measured the TPA spectrum using the pump and probe technique at time  $t=0$ . In this technique the linearly polarized pump beam from the low-repetition high-power laser system was set *fixed* at 1.55 eV, that is below the polymer main absorption band; whereas the probe beam from the white light supercontinuum beam spreads the pump-probe spectral range from 1.6 to 2.6 eV; thus covering the TPA photon energy range from 3.15 to 4.15 eV. If only linear absorption is considered, then the pump beam alone is unable to generate photoexcitations, since its photon energy at 1.55 eV is much lower than the DPA optical gap at  $\sim 2.8$  eV. However the temporal and spatial overlap between the pump and probe beams on the DPA film leads to a transient PA signal that peaks at  $t=0$ . As seen in Fig. 4 for a pump at 1.55 eV and probe at  $\sim 1.9$  eV, this PA has a temporal profile identical to the cross-correlation function of the pump and probe pulses, and thus we interpret it as due to TPA of one pump photon with one probe photon. We note that, in principle, it is also possible to obtain TPA from the mid-IR laser system, for  $\hbar\omega$  (pump) at 3.1 eV and  $\hbar\omega$  (probe) in resonance with the most strongly coupled  $mA_g$



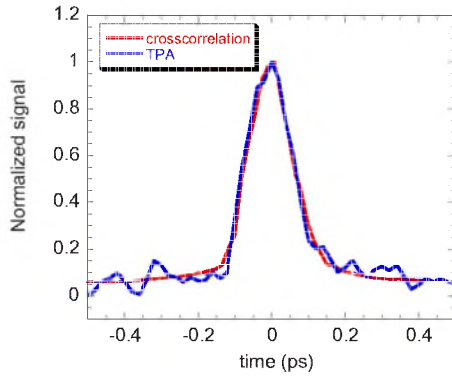


FIG. 4. (Color online) DPA transient TPA trace (blue line) involving the pump (at 1.55 eV) and probe (at 1.9 eV) pulses, compared to the pump-probe cross-correlation trace (red line) measured using a NLO crystal.

state. However from the transient PM decay measurements (see below) we conclude that the contribution of TPA to the mid-IR PM spectrum is negligible small.

Figure 5 shows the TPA spectrum of a DPA film obtained by the pump-probe technique up to 4.2 eV, compared with the linear-absorption spectrum. The TPA spectrum shows a broad band (full width at half maximum of  $\sim 0.4$  eV) that peaks at 3.4 eV with a prominent shoulder extending to 4 eV. We interpret the TPA spectrum in DPA as a superposition of three contributions: the TES at 3.3 eV,  $mA_g$  state at 3.5 eV, and  $kA_g$  state at 3.9 eV;<sup>37,43,44</sup> these states are in agreement with the EA spectrum discussed above. The dashed lines in Fig. 5 represent the individual contributions of these three states; their sum (red solid line) fits the experimental TPA spectrum very well. We conclude that the TPA spectrum contains a substantial component at 3.3 eV that is close in energy to band B in the linear-absorption spectrum, which we interpreted above as due to  $1A_g \rightarrow TES$  transition. This is in agreement of the dual parities assigned to the TES band. It contains degenerate states with odd and even parities, respectively, which contribute to both absorption and TPA spectra. The higher energy TPA bands, namely, the  $mA_g$  and  $kA_g$  are in agreement with TPA spectra of other PCPs.<sup>26</sup> Also the energy difference between the prominent bands in the linear-absorption and TPA spectra of  $\sim 0.5$  eV sets a lower limit for the exciton binding energy in this polymer, in agreement

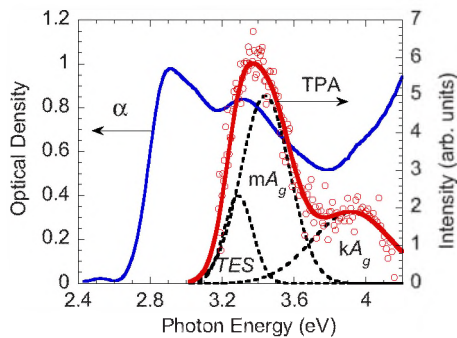


FIG. 5. (Color online) The TPA spectrum of DPA (red circles) compared to the linear-absorption spectrum (blue line). The states TES,  $mA_g$ , and  $kA_g$  are assigned.

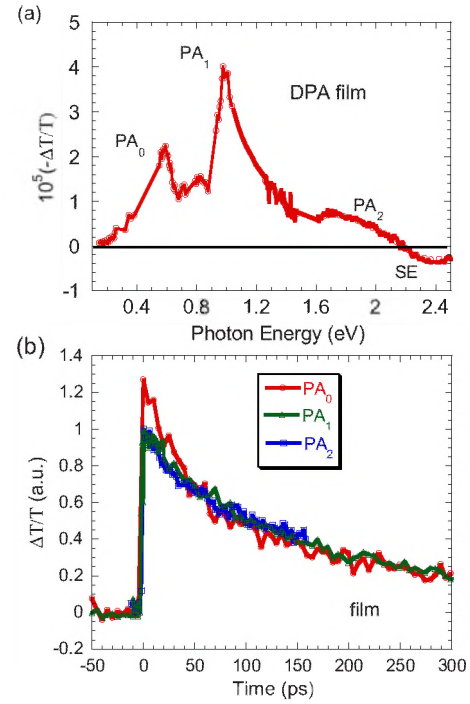


FIG. 6. (Color online) (a) The transient PM spectrum of DPA film at  $t=0$  ps. The PA bands PA<sub>0</sub>, PA<sub>1</sub>, PA<sub>2</sub>, and SE are assigned. (b) The transient decay dynamics of the main PA bands assigned in (a).

with  $E_b$  ( $\sim 1$  eV) extracted above from the EA spectrum.

#### D. Transient photomodulation spectroscopy

Figures 6(a) and 7(a) show the transient PM spectrum of DPA film and dilute solution, respectively, at  $t=0$  ps. Both PM spectra contain three PA bands: PA<sub>0</sub> at  $\sim 0.6$  eV, PA<sub>1</sub> at  $\sim 0.9$  eV, and a broad PA<sub>2</sub> band in the near-IR spectral range; the PM spectra also contain a strong SE band peaked at  $\sim 2.6$  eV. All PA bands show approximately the same decay dynamics [Figs. 6(b) and 7(b)], and therefore originate from the same photoexcitation species. Since the SE is part of this species characteristic, we therefore identify it as intrachain singlet exciton or  $1B_u$ . The PA<sub>1</sub> and PA<sub>2</sub> bands are consequently interpreted as optical transitions from the relaxed  $1B_u \rightarrow mA_g$  and  $1B_u \rightarrow kA_g$ , respectively, similar to excitons in other PCPs.<sup>23</sup> However PA<sub>0</sub> does not occur in the PM spectrum of excitons in other PCPs. We therefore propose that PA<sub>0</sub> is due to the optical transition from the relaxed  $1B_u$  to the TES, that is also absent in other PCPs. We note that the energy difference between PA<sub>0</sub> and PA<sub>1</sub> bands ( $\sim 0.4$  eV) is larger than the energy difference ( $\sim 0.2$  eV) between the TES state and  $mA_g$  that we deduced above from the TPA spectrum. Although the two transitions are to the same final state: we emphasize that both PA<sub>0</sub> and PA<sub>1</sub>, in fact, involve excited state transitions, namely,  $1B_u \rightarrow TES$  and  $1B_u \rightarrow mA_g$ , respectively, whereas the TPA spectrum reflects transitions  $1A_g \rightarrow TES$  and  $1A_g \rightarrow mA_g$ , where the ground state is involved. Thus, the discrepancy in the relative energies of the two PA bands compared to the two TPA bands may reflect the different electronic relaxation state pa-

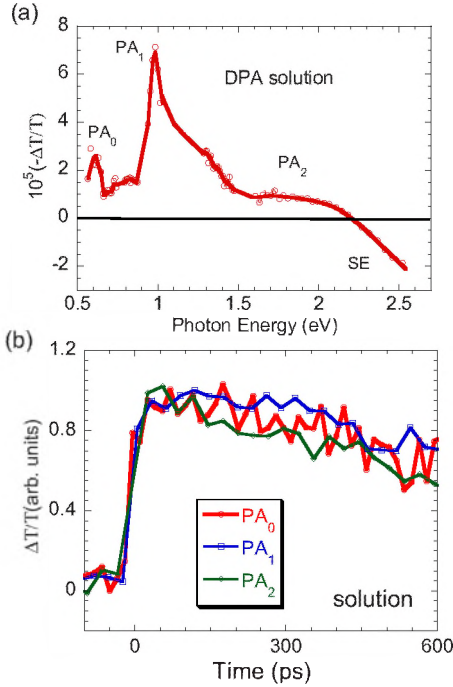


FIG. 7. (Color online) Same as in Fig. 6, but for a DPA dilute solution.

rabolas in the individual configuration coordinate space of  $1A_g$  and  $1B_u$ , respectively.<sup>36</sup> We note that the Frank-Condon overlap (which is determined by the excited state parabolas) dominates the phonon side bands in the optical transitions, and this, in fact, determines the peak position of the optical transition. We also note that the transient PM spectrum of the DPA film down to 0.13 eV does not show any other important band, such as due to IR-active vibrations that are related to charge photogeneration.<sup>10,45</sup> This is in agreement with the assignment of the three PA bands as due to transitions involving intrachain excitons.

#### IV. SUMMARY

We used a variety of linear and nonlinear optical spectroscopies for studying the excited states and photoexcitations of the interesting polymer DPA that has a degenerate ground state. The NLO spectroscopies include electroabsorption, two-photon absorption, and ultrafast photomodulation; whereas the linear spectroscopies were PL emission and absorption. We found that the DPA NLO spectra are dominated by five essential excited states. These are the odd parity exciton states  $1B_u$  and  $nB_u$ ; the even parity exciton states  $mA_g$  and  $kA_g$ ; and an excited band of states with even and odd parities, namely, the TES, with its transition dipole moment from the  $1B_u$  is mainly perpendicular to the polymer chain direction. The energies of these important states obtained in our study are summarized in Fig. 8; this picture is very different from the excited state picture of other, more conventional PCPs. Including the  $1A_g$ , all six states contribute to the EA spectrum; but only the TES and two  $A_g$  states are seen in the TPA spectrum and PA transitions from the excited  $1B_u$

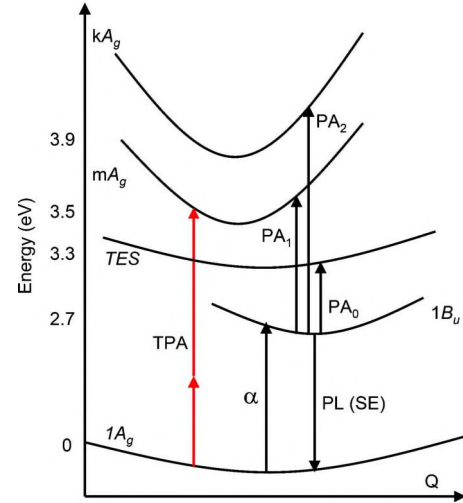


FIG. 8. (Color online) The most important intrachain energy states and allowed optical transitions for DPA. The PA bands are excited state absorptions;  $\alpha$  and TPA is linear and NLO absorption, respectively, and PL may be replaced by SE in the pump-probe experiment.

exciton to upper states obtained in the transient PM spectrum.

The comparison between the TPA and linear-absorption spectra show that the two spectra peaks at energies  $\sim 0.5$  eV apart; in fact the TPA gets a *minimum* at the energy of the linear-absorption peak. This shows that the electron-electron interaction dominates the characteristic properties of the excited states in DPA. Therefore is not surprising that the primary photoexcitations in DPA are singlet excitons with substantial PL emission efficiency. The singlet excitons in DPA are characterized by three strong PA bands in the mid- and near-IR spectral range, and a SE band in the visible spectral range. Also the EA spectrum does not contain any FK oscillation at the continuum band edge, but instead shows derivativelike features of the main excitons. The EA polarization anisotropy in DPA films is unusual and is governed by the polarization properties of the TES that is unique to this polymer.

#### ACKNOWLEDGMENTS

This work was supported in part by the NSF under Grant No. DMR 08-03325 and the DOE under Grant No. 05-03172 at the University of Utah. C.-X S. thanks the NUST “Zijin star” project and NUST Research Funding No. 2010ZDJH03.

#### APPENDIX

##### Polarization anisotropy of the EA spectrum in DPA films

Electroabsorption can be described by the third-order optical susceptibility, namely,  $\chi^{(3)}(-\omega; \omega, 0, 0)$ .<sup>33,38</sup>

$$-\Delta T/T = \frac{4\pi\omega}{nc} \text{Im}[\chi^{(3)}(-\omega; \omega, 0, 0)] F^2 d, \quad (\text{A1})$$

where  $d$  is the film thickness,  $n$  is the refractive index,  $c$  is the speed of light, and  $\omega$  is the optical frequency; the field

modulation  $f \ll \omega$ , and this explains the zero frequency in the bracket of  $\chi^{(3)}$  in Eq. (A1). The relation between the EA and  $\chi^{(3)}$  in Eq. (A1) shows that the polarization dependence of the EA spectrum is, in fact, related to the anisotropy of the  $\chi_{mnkl}^{(3)}$  tensor in PCPs.

The  $\chi^{(3)}$  spectrum may be calculated using the SOS model.<sup>25,33,38</sup> In this model as applied to PCPs, there are usually four main classes of terms [(a)–(d)],<sup>25,26</sup> which indicate the channel taken by the dipole-moment transitions. One such class, (a) is the channel ( $1A_g \rightarrow 1B_u \rightarrow 1A_g \rightarrow 1B_u \rightarrow 1A_g$ ) that involves only the  $1A_g$  and  $1B_u$  states. Channel (b) involves the transition  $1A_g$  to  $nB_u$  ( $1A_g \rightarrow nB_u \rightarrow 1A_g \rightarrow nB_u \rightarrow 1A_g$ ). Channel (c) involves both  $1B_u$  and  $mA_g$  ( $1A_g \rightarrow 1B_u \rightarrow mA_g \rightarrow 1B_u \rightarrow 1A_g$ ). Whereas channel (d) involves *all four* essential states via the process  $1A_g \rightarrow 1B_u \rightarrow mA_g \rightarrow nB_u \rightarrow 1A_g$ .

In DPA, since the additional TES band state processes both odd and even parities, five additional channels may be considered in calculating  $\chi^{(3)}$  spectrum. These are: (e) ( $1A_g \rightarrow TES \rightarrow 1A_g \rightarrow TES \rightarrow 1A_g$ ); (f) ( $1A_g \rightarrow TES \rightarrow mA_g \rightarrow TES \rightarrow 1A_g$ ); (g) ( $1A_g \rightarrow 1B_u \rightarrow TES \rightarrow 1B_u \rightarrow 1A_g$ ); (h)  $1A_g \rightarrow TES \rightarrow mA_g \rightarrow nB_u \rightarrow 1A_g$ ; and (i) ( $1A_g \rightarrow 1B_u \rightarrow TES \rightarrow nB_u \rightarrow 1A_g$ ). It has been proven that channel (c) dominates the calculated  $\chi^{(3)}$  spectrum in 2-methoxy-5-(2'-ethylhexyloxy) (MEH)-PPV (Ref. 25) and PFO.<sup>26</sup> Thus for simplicity we discuss here the polarization dependence of channel (c) and corresponding channel (f). The contribution to the polarization dependence of  $\chi_{mnkl}^{(3)}$  from channels (c) and (f) can be expressed as  $K\mu_{01m}\mu_{12n}\mu_{21k}\mu_{10l}D_c$  and  $K\mu_{01'm}\mu_{1'2n}\mu_{21'k}\mu_{1'0l}D_f$ , respectively.  $\mu_{ij}$  is the strength of the dipole-moment transition from state  $i$  to state  $j$ , where the 0, 1, 1', and 2 with index  $i$  or  $j$  stands for  $1A_g$ ,  $1B_u$ , TES, and  $mA_g$ , respectively. The indices  $m, n, k$ , and  $l$  are either  $x$  or  $y$ ; and the  $D_c$  and  $D_f$  terms, each represents four terms with energy denominators that depend on the photon energy. The factor  $K$  is a result of intrinsic permutation symmetry requirements.<sup>25,26</sup>

In channel (c) all transition dipoles are along to the polymer chain; thus  $\mu_{ijx}$  may be expressed as  $\mu_{ij} \cos(\theta)$ , and

consequently  $\mu_{ijy}$  may be expressed as  $\mu_{ij} \sin(\theta)$ , where  $\theta$  is the angle between the polymer chain and the applied electrical field direction, assumed to be in the  $x$  direction. However in channel (f)  $\mu_{01'}$  and  $\mu_{1'2}$  are transversal and longitudinal to the polymer chain, respectively,<sup>19,20</sup> therefore  $\mu_{01'x} = \mu_{01'} \sin(\theta)$ ,  $\mu_{01'y} = \mu_{01'} \cos(\theta)$ ,  $\mu_{1'2x} = \mu_{1'2} \cos(\theta)$ , and  $\mu_{1'2y} = \mu_{1'2} \sin(\theta)$ . When the polarization is parallel to the applied electric field direction, only  $\chi_{xxxx}$  needs be considered. In addition when the light polarization is perpendicular to the applied electric field direction, there are two other contributions, namely,  $\chi_{yyxx}$  and  $\chi_{yxyx}$ . In contrast to the situation in pump/probe measurements, where  $\chi_{yxyx}$  is integrated in time to be zero;<sup>46</sup> in EA, since the applied electric field here is constant in time the  $\chi_{yxyx}$  contribution to the EA signal cannot be neglected. The EA depolarization ratio,  $\rho$ , can be then calculated from the relation

$$\rho = 2\chi_{xxxx}/(\chi_{yyxx} + \chi_{yxyx}). \quad (A2)$$

The average of  $\chi_{xxxx}$ ,  $\chi_{yyxx}$ , and  $\chi_{yxyx}$  for channel (c) and channel (f), respectively, over the chain direction distribution (assumed to be isotropic in space) is proportional to the integrals  $\int \cos^4 \theta d\theta$ ,  $\int \sin^2 \theta \cos^2 \theta d\theta$ ,  $\int \sin^2 \theta \cos^2 \theta d\theta$ , and  $\int \sin^2 \theta \cos^2 \theta d\theta$ ,  $\int \sin^2 \theta \cos^2 \theta d\theta$ , and  $\int \cos^4 \theta d\theta$ . Therefore from Eq. (A2) we calculate the EA depolarization ratio,  $\rho$ , for channel (c) and channel (f) to be 3 and 0.5, respectively. We note that for channel (e), since only one transition dipole is considered, there is no difference between parallel and perpendicular EA after averaging over the randomly distributed polymer chains. The depolarization ratio of channel (g) is the same as that of channel (f). For channels (h) and (i) the transition from  $1A_g$  to  $nB_u$  around 4 eV was assigned as charge-transfer transition of which dipole moment is also perpendicular to the polymer backbone;<sup>20</sup> thus channels (h) and (i) share the same polarization dependence as that of channel (f). Therefore, except channel (e), all others channels involving the TES state present unusual polarization dependence, which qualitatively explained the polarized EA measurements for  $\hbar\omega > 3.2$  eV in DPA film.

\*Present address: Center for Polymers and Organic Solids, University of California, Santa Barbara, California, USA.

†Author to whom correspondence should be addressed; val@physics.utah.edu

<sup>1</sup> *Handbook of Conducting Polymers*, 2nd ed., edited by T. A. Skotheim, R. L. Elsenbaumer, and J. R. Reynolds (Marcel Dekker, New York, 1998).

<sup>2</sup> *Ultrafast Dynamics and Laser Action of Organic Semiconductors*, edited by Z. Vally Vardeny (Taylor & Francis, London/CRC Press, Boca Raton, 2008).

<sup>3</sup> *Primary Photoexcitations in Conjugated Polymers: Molecular Exciton versus Semiconductor Band Model*, edited by S. Saricifci (World Scientific, Singapore, 1997).

<sup>4</sup> L. Rothberg, in *Semiconducting Polymers: Chemistry, Physics and Engineering*, edited by G. Hadzioannou and G. G. Malli-

aras (Wiley, New York, 2006), Vol. I, pp. 179–204, and references therein.

<sup>5</sup> S. Singh, T. Drori, and Z. V. Vardeny, *Phys. Rev. B* **77**, 195304 (2008).

<sup>6</sup> P. Miranda, D. Moses, and A. J. Heeger, *Phys. Rev. B* **70**, 085212 (2004).

<sup>7</sup> D. Psichos and S. Mazumdar, *Phys. Rev. B* **79**, 155106 (2009).

<sup>8</sup> H. Shirakawa, T. Masuda, and K. Takeda, in *The Chemistry of Triple-Bonded Functional Groups*, edited by S. Patai (Wiley, New York, 1994).

<sup>9</sup> T. Masuda, T. Hamano, K. Tsuchihara, and T. Higashimura, *Macromolecules* **23**, 1374 (1990).

<sup>10</sup> I. Gontia, S. V. Frolov, M. Liess, E. Ehrenfreund, K. Tada, H. Kajii, R. Hydayat, A. Fujii, K. Yoshino, M. Teraguchi, and T. Masuda, *Phys. Rev. Lett.* **82**, 4058 (1999).

<sup>11</sup> A. J. Heeger, K. Kivelson, J. S. Schrieffer, and W. P. Su, *Rev.*



- Mod. Phys.* **60**, 781 (1988).
- <sup>12</sup>K. Tada H. Sawada, J. Kyokane and K. Yoshino, *Jpn. J. Appl. Phys., Part 2* **34**, L1083 (1995).
  - <sup>13</sup>S. V. Frolov, A. Fujii, D. Chinn, M. Hirohata, R. H. Masahiro T. Masuda, K. Yoshino, Z. V. Vardeny, *Adv. Mater.* **10**, 869 (1998).
  - <sup>14</sup>Z. G. Soos and S. Ramasesha, *Phys. Rev. B* **29**, 5410 (1984).
  - <sup>15</sup>P. Tavan and K. Schulten, *Phys. Rev. B* **36**, 4337 (1987).
  - <sup>16</sup>A. Shukla and S. Mazumdar, *Phys. Rev. Lett.* **83**, 3944 (1999).
  - <sup>17</sup>A. Shukla, *Chem. Phys.* **300**, 177 (2004); *Phys. Rev. B* **69**, 165218 (2004).
  - <sup>18</sup>A. Shukla and P. Sony, *Synth. Met.* **155**, 368 (2005).
  - <sup>19</sup>H. Ghosh, A. Shukla, and S. Mazumdar, *Phys. Rev. B* **62**, 12763 (2000).
  - <sup>20</sup>I. I. Gontia, Z. V. Vardeny, T. Masuda, and K. Yoshino, *Phys. Rev. B* **66**, 075215 (2002).
  - <sup>21</sup>L. Lüer, C. Manzoni, G. Cerullo, G. Lanzani, and Z. V. Vardeny, *Chem. Phys. Lett.* **444**, 61 (2007).
  - <sup>22</sup>S. V. Frolov, Z. Bao, M. Wohlgenannt, and Z. V. Vardeny, *Phys. Rev. B* **65**, 205209 (2002).
  - <sup>23</sup>H. Zhao, S. Mazumdar, C.-X. Sheng, M. Tong, and Z. V. Vardeny, *Phys. Rev. B* **73**, 075403 (2006), and references therein.
  - <sup>24</sup>C.-X. Sheng, M. Tong, S. Singh, and Z. V. Vardeny, *Phys. Rev. B* **75**, 085206 (2007).
  - <sup>25</sup>M. Liess, S. Jeglinski, Z. V. Vardeny, M. Ozaki, K. Yoshino, Y. Ding, and T. Barton, *Phys. Rev. B* **56**, 15712 (1997).
  - <sup>26</sup>M. Tong, C.-X. Sheng, and Z. V. Vardeny, *Phys. Rev. B* **75**, 125207 (2007).
  - <sup>27</sup>A. Fujii, R. Hidayat, T. Sonoda, T. Fujisawa, M. Ozaki, Z. V. Vardeny, M. Teraguchi, T. Masuda, and K. Yoshino, *Synth. Met.* **116**, 95 (2001).
  - <sup>28</sup>C. J. Collison, L. J. Rothberg, C. Tremaneckarn, and Y. Li, *Macromolecules* **34**, 2346 (2001).
  - <sup>29</sup>R. Hidayat, S. Tatsuhara, D. W. Kim, M. Ozaki, K. Yoshino, M. Teraguchi, and T. Masuda, *Phys. Rev. B* **61**, 10167 (2000).
  - <sup>30</sup>*Semiconductors and Semimetals*, edited by R. K. Willardson and A. C. Beer (Academic Press, New York, 1972), Vol. 9.
  - <sup>31</sup>L. Sebastian, G. Weiser, and H. Bassler, *Chem. Phys.* **61**, 125 (1981).
  - <sup>32</sup>G. Weiser, *Phys. Rev. B* **45**, 14076 (1992).
  - <sup>33</sup>D. Guo, S. Mazumdar, S. N. Dixit, F. Kajzar, F. Jarka, Y. Kawabe, and N. Peygamparian, *Phys. Rev. B* **48**, 1433 (1993).
  - <sup>34</sup>L. Sebastian and G. Weiser, *Phys. Rev. Lett.* **46**, 1156 (1981).
  - <sup>35</sup>T. A. Kulakov and D. Y. Paraschuk, *Chem. Phys. Lett.* **325**, 517 (2000).
  - <sup>36</sup>S. V. Frolov, M. Liess, P. A. Lane, W. Gellermann, Z. V. Vardeny, M. Ozaki, and K. Yoshino, *Phys. Rev. Lett.* **78**, 4285 (1997).
  - <sup>37</sup>However there might be a contradiction between the exciton description of DPA and the possibility of ferroelectricity in this polymer; S. Brazovskii and N. Kirova, *Synth. Met.* (to be published).
  - <sup>38</sup>S. N. Dixit, D. Guo, and S. Mazumdar, *Phys. Rev. B* **43**, 6781 (1991).
  - <sup>39</sup>B. J. Orr and J. F. Ward, *Mol. Phys.* **20**, 513 (1971).
  - <sup>40</sup>M. Chandross, S. Mazumdar, M. Liess, P. A. Lane, Z. V. Vardeny, and K. Yoshino, *Phys. Rev. B* **55**, 1486 (1997).
  - <sup>41</sup>M. J. Rice and Yu. N. Garstein, *Phys. Rev. Lett.* **73**, 2504 (1994).
  - <sup>42</sup>A. Chakrabarti and S. Mazumdar, *Phys. Rev. B* **59**, 4839 (1999).
  - <sup>43</sup>P. Sony and A. Shukla, *Phys. Rev. B* **71**, 165204 (2005).
  - <sup>44</sup>P. Najeckalski, Y. Morel, O. Stephan, and P. L. Baldeck, *Chem. Phys. Lett.* **343**, 44 (2001).
  - <sup>45</sup>P. B. Miranda, D. Moses, and A. J. Heeger, *Phys. Rev. B* **64**, 081201 (2001).
  - <sup>46</sup>Z. Vardeny and J. Tauc, *Opt. Commun.* **39**, 396 (1981).